Proceedings of the 9th World Congress on Mechanical, Chemical, and Material Engineering (MCM'23)
Brunel University, London, United Kingdom –August 06-08, 2023
Paper No. 122
DOI: 10.11159/htff23.122

Three Dimensional CFD Analyses for the Effect of Solid Concentration on Gas Holdup in a Slurry Bubble Column

M. W. Abdulrahman[1], N. Nassar[2]
[1]Rochester Institute of Technology (RIT)
Dubai, UAE
mwacad@rit.edu; nin8507@g.rit.edu
[2]Rochester Institute of Technology (RIT)
Dubai, UAE

Abstract – In this paper, 3D-CFD simulations are used to model solid particle concentration effects on the hydrodynamic behavior of a direct contact heat transfer slurry bubble column reactor containing helium gas and a slurry of liquid water and solid alumina particles. The results of this paper are compared to previous experimental data and shows a maximum error of 8.37% for a solid particle concentration of 10%, while the errors are decreasing when the solid particle concentration is decreased. Also, It is shown that decreasing solid particle concentration increases gas holdup, where increasing solid concentration from 0% to 10% leads to a decrease in gas holdup by 6%. Moreover, the results of this paper are compared to previous 2D CFD results and shows better accuracy, where the maximum error of the 2D CFD simulations were 28.5%.

Keywords**:** gas holdup; hydrodynamics; solid concentration; CFD; 3D

1. Introduction

The Cu-Cl cycle, which involves the production of hydrogen, has been recognized as a highly favorable low temperature cycle [1, 2]. The Cu-Cl cycle of hydrogen production involves an oxygen reaction that necessitates a high temperature heat source. High-temperature heat can be produced through the utilization of non-polluting sources such as nuclear reactors or solar thermal energy. Various heat transfer mechanisms for the oxygen reactor have been examined through prior research [3-7]. The optimal heat transfer mechanism for the oxygen reactor has been established to be direct contact heat transfer from the oxygen gas to the molten CuCl [7-9]. The present technique involves the heating of a portion of the oxygen gas produced during the decomposition process of the oxygen reactor to a temperature of 530ºC, followed by its return into the oxygen reactor. This facilitates the transfer of heat directly to the molten salt.

Studies on bubble column reactors have been conducted via experimental and numerical methods over time. Abdulrahman et al. [9] conducted a review of the Eulerian methodology utilized in computational fluid dynamics (CFD) analyses for bubble column reactors. The outcomes of 2D computational fluid dynamics (CFD) analyses for the gas holdup, volumetric heat transfer coefficient, gas and slurry temperatures, and solid concentration of the bubble column reactor have been investigated by Abdulrahman [10-14]. The study conducted by Abdulrahman [14] aimed to examine the impact of different solid concentrations, specifically 0%, 5%, and 10% of solid Alumina, on gas holdup in a bubble column reactor. The reactor consisted of liquid water and helium gas. The investigation was carried out utilizing a two-dimensional computational fluid dynamics (CFD) analysis. A multiphase Eulerian model was used to create the system, incorporating a viscous-standard $k-\varepsilon$ turbulence model. The findings show that an increase in the concentration of solid particles leads to a decrease in gas holdup.

Zhou et al. [15] analyzed the effects of particles on a gas liquid flows in a slurry bubblecolumn using a conceptual model. The particle dependent dual bubble size (PDBS) model was created to investigate the effects of viscosity and density changes due to the addition of particles,as well as the change to the bubble drag coefficient due to presence of particles. The model was a three-phase model composing of air, water, and glass beads. When consideringthe effects of viscosity and density it was observed that there was a higher level of stability with increased slurry viscosity and density. This was apparent as there was a delay in the flow regime transition to a higher flow rate. Overall, it was concluded that the increase in solid concentration will result in a decrease of thegas holdup.

Wodolazski [16], generated a 3D CFD simulation of a slurry bubble column reactor toanalyze the flow of syngas in a 3-phase flow (syngas, paraffin oil, solid particles). A Eulerian- Eulerian approach was used with a $k-\varepsilon$ turbulence model. Parameters analyzed in this study included the superficial gas velocity, initial solid particle concentration (10%, 30% and

50%), gasholdup, and bubble size distribution. The report concluded that increasing the slurry concentration leads to a decrease in axial gas holdup. Additionally, the increase of the slurry concentration leads to a decrease in the bubble breakup rate. An approximate parabolic relationship was observed between the effects of the gas velocity and the axial solids holdup profile.

2. CFD Simulation Model

The simulations presented in this study have been verified through comparison with the experimental results created by Abdulrahman [8, 17-20]. The simulated reactor has been designed in a manner that simplifies the physical reactor shown in Fig. 1 to minimize computational costs.

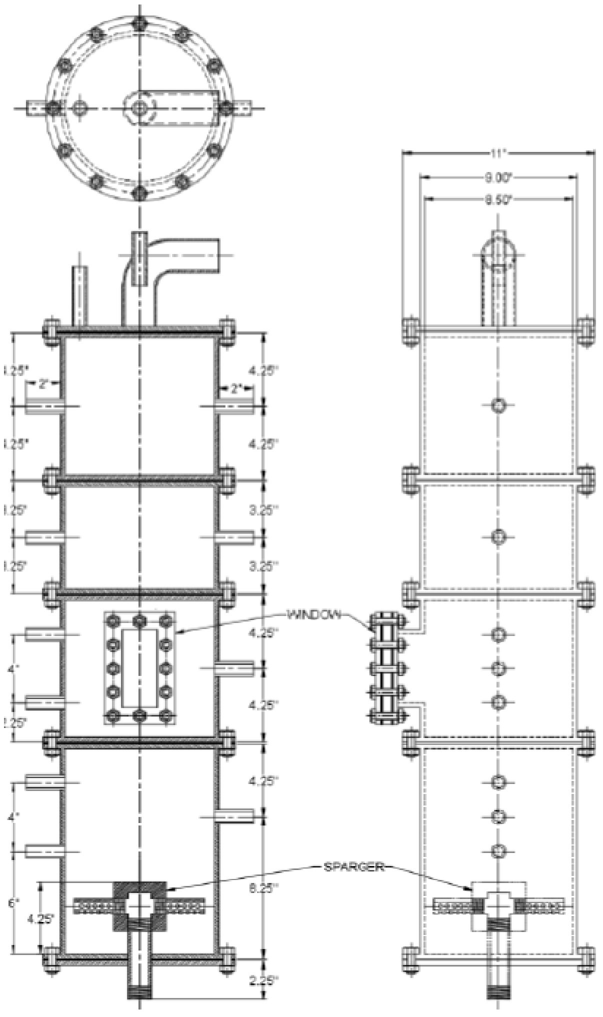

Fig.1 Design diagram of the experimental slurry bubble column reactor [8].

Abdulrahman conducted his experiments on a Water-Helium-Alumina system as a result of the challenges associated with Cuprous Chloride (CuCl) and Oxygen (O_2) substances [8, 17-20]. The difficulties include the difficulty in detecting O_2 bubbles in molten CuCl owing to its dark color, the corrosive properties of the CuCl molten salt, and the tendency of O_2 gas to oxidize different substances, thereby accelerating its combustion [8, 21-22]. Abdulrahman has found that using liquid water at 22°C and Helium gas at 90°C can replace the molten CuCl at 530°C and oxygen gas at 600°C to give the same hydrodynamics and heat transfer behaviors [8]. The present study involves the utilization of a Eulerian-Eulerian model, a Eulerian sub-model, and a pressure-based solver type for conducting simulations of a 3D plane system. The employed turbulence model is the RNG k-ε model, while the standard wall function is utilized as the wall function. A hexahedral mesh is utilized for the BCR, as shown in Fig. 2. The mesh's independence analyses are conducted to ensure that the optimal mesh size is selected, which balances computational expenses with satisfactory outcomes. The ultimate configuration of the mesh is comprised of 26,825 nodes and 24,396 elements. The utilization of finer meshes led to a 3% variation in gas holdup. The inlet boundary condition is defined by an inlet superficial gas velocity and a gas holdup of 1. The outlet pressure is adjusted to match the pressure of the atmosphere. The reactor walls are subjected to a no-slip condition in both phases. The estimation of turbulent kinetic energy and dissipation rate at the inlet and outlet represents a significant challenge. Therefore, a total of 5,000 iterations were employed to accurately determine these parameters. Table 1 presents the equations utilized in the computational fluid dynamics (CFD) investigation outlined in this paper. The equations presented in Table 1 are solely formulated for the gaseous state. Given the similarity between the equations for liquid phase and those for gas phase, the former is not repeated.

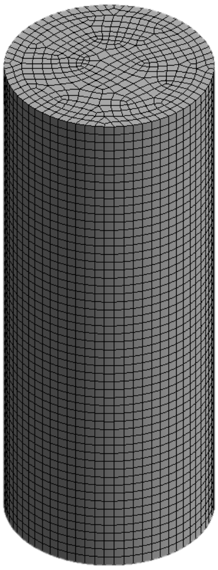

Fig.2 hexahedron mesh of slurry bubble column.

Table 1: Details of equations used in the 3D CFD simulations.

Description [reference]	**Equation**
equation [23]	$\alpha_g \, dV$
ity equation in 3D Polar coord	$\frac{\partial v_{r,g}}{\partial r} + \frac{v_{r,g}}{r} + \frac{1}{r}\frac{\partial v_{\theta,g}}{\partial \theta} + \frac{\partial v_{y,g}}{\partial y} = 0$
um equation in 3D Polar co	$+ v_r \frac{\partial v_r}{\partial r} + \frac{v_\theta}{r}\frac{\partial v_r}{\partial \theta} + vy\frac{\partial v_r}{\partial y} - \frac{v_\theta^2}{r}) = -\alpha_g \frac{\partial P}{\partial r} + \alpha_g \frac{\mu_{g,eff}}{3}\frac{\partial(\nabla.V)}{\partial r} +$ $g[\frac{1}{r}\frac{\partial}{\partial r}(r\frac{\partial v_r}{\partial r}) + \frac{1}{r^2}\frac{\partial^2 v_r}{\partial \theta^2} + \frac{\partial^2 v_r}{\partial y^2} - \frac{v_r}{r^2} - \frac{2}{r^2}\frac{\partial v_\theta}{\partial \theta}] + \rho_g \alpha_g \, g_r + M_{i,g,r}$ $+ v_r \frac{\partial v_\theta}{\partial r} + \frac{v_\theta}{r}\frac{\partial v_\theta}{\partial \theta} + v_y \frac{\partial v_\theta}{\partial y} + \frac{v_r v_\theta}{r}) = -\alpha_g \frac{1}{r}\frac{\partial P}{\partial \theta} + \alpha_g \frac{\mu_{g,eff}}{3r}\frac{\partial(\nabla.V)}{\partial \theta} +$ $[\frac{1}{r}\frac{\partial}{\partial r}(r\frac{\partial v_\theta}{\partial r}) + \frac{1}{r^2}\frac{\partial^2 v_\theta}{\partial \theta^2} + \frac{\partial^2 v_\theta}{\partial y^2} + \frac{2}{r^2}\frac{\partial v_r}{\partial \theta} - \frac{v_\theta}{r^2}] + \rho_g \alpha_g \, g_\theta + M_{i,g,\theta}$ $+ v_r \frac{\partial v_y}{\partial r} + \frac{v_\theta}{r}\frac{\partial v_y}{\partial \theta} + v_y \frac{\partial v_y}{\partial y}) = -\alpha_g \frac{\partial P}{\partial y} + \alpha_g \, \mu_{g,eff}[\frac{1}{r}\frac{\partial}{\partial r}(r\frac{\partial v_y}{\partial r}) + \frac{1}{r^2}\frac{\partial^2 v_y}{\partial \theta^2}$ $\alpha_g g_y + M_{i,g,y}$

equation in 3D Polar coordina	$\frac{\partial T_g}{\partial t} + v_{r,g}\frac{\partial T_g}{\partial r} + \frac{v_{\theta,g}}{r}\frac{\partial T_g}{\partial \theta} + v_{y,g}\frac{\partial T_g}{\partial y}) = \bar{\bar{\tau}}_g : \nabla V_g + k_g(\frac{1}{r}\frac{\partial}{\partial r}(r\frac{\partial T_g}{\partial r}) + \frac{1}{r^2}\frac{\partial^2 Tg}{\partial \theta^2}$ $S_g + Q_{g,sl}$	
e density	ρ_g	
rce [23]	$\frac{f}{\tau_b}\, d_b\, A_i\, (\boldsymbol{V_g} - \boldsymbol{V_l})$	
al area [23]	$\frac{g\,(1-\alpha_g)}{d_b}$	
-Naumann drag equation [24]	$\frac{4\,(1+0.15\,Re_b^{0.687})}{Re_b}$	$Re_b \leq 1000$
	.44	$Re_b > 1000$

3. Results

The 3D curve in Fig. 3 shows the relationship between the gas holdup and the variables C_s and U_{gs}. Figure 4 illustrates the impact of different values of C_s on α_g, as the superficial gas velocity (U_{gs}) is changed in a Helium-Water-Alumina bubble column. Figures 5 and 6 depict the outlines of the cut section of the BCR, which was extracted from the central regions of the XY and ZY planes, respectively. In order to achieve a more accurate profile of α_g, further sections were extracted from the ZX plane within the reactor at varying heights of 10, 20, and 30 cm from the base of the reactor. The asymmetry of the gas holdup in the XY, ZY, and ZX planes is apparent from the contours, suggesting that its behavior exhibit significant three-dimensional characteristics. An inverse relationship between α_g and C_s is noted, whereby an increase in C_s results in a decrease in α_g. At a superficial gas velocity of 0.05 m/s, when the concentration is raised from $C_s = 0\%$ to $C_s = 10\%$, the gas holdup experiences a reduction of approximately 6% while the static liquid height (H) equals 45 cm. At a superficial gas velocity of 0.15m/s and a static liquid height of 55cm, an increase in the C_s from 0% to 10% results in a 14% decrease in gas holdup. This phenomenon is noted as a result of the direct relationship between the concentration of solid particles and the viscosity of the slurry. Elevated viscosity levels result in the formation of large gas bubbles and diminish the occurrence of bubble breakage due to interfacial instabilities. The high-rise velocity of large bubbles will result in a decrease in gas holdup [25].

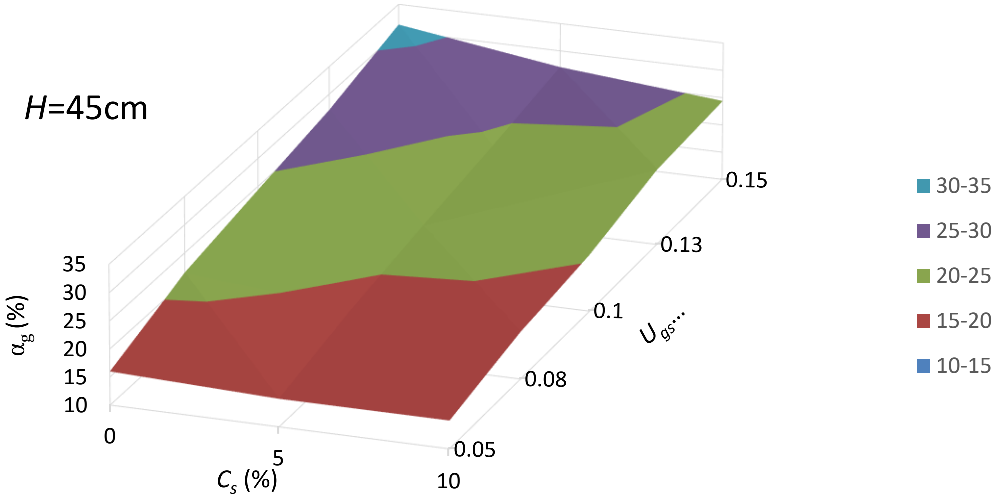

Fig.3 Average gas holdup versus solid particle concentration and superficial gas velocity.

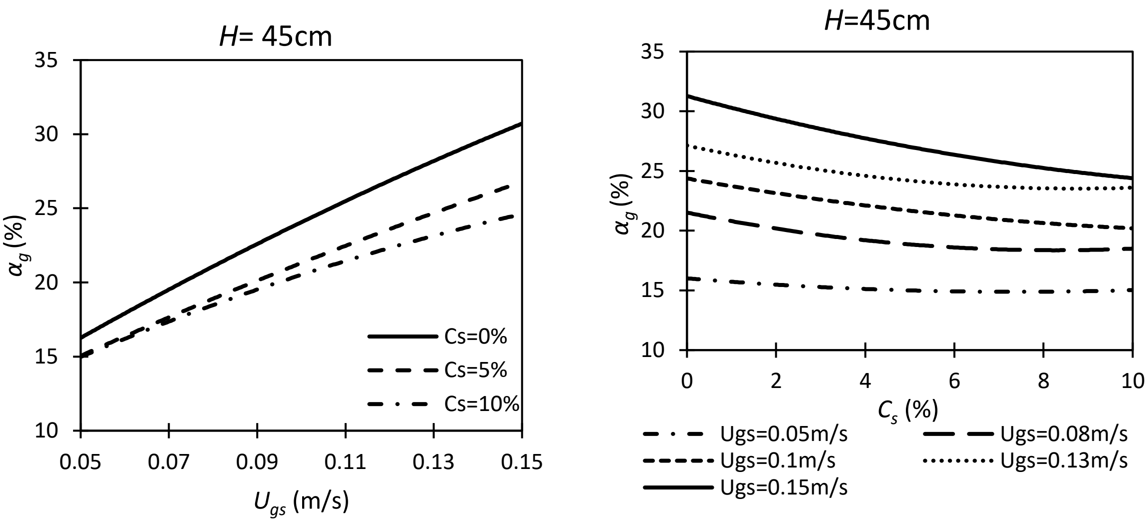

(a)

(b)

Fig. 4 The effect of solid particle concentration on gas holdup for different superficial gas velocities.

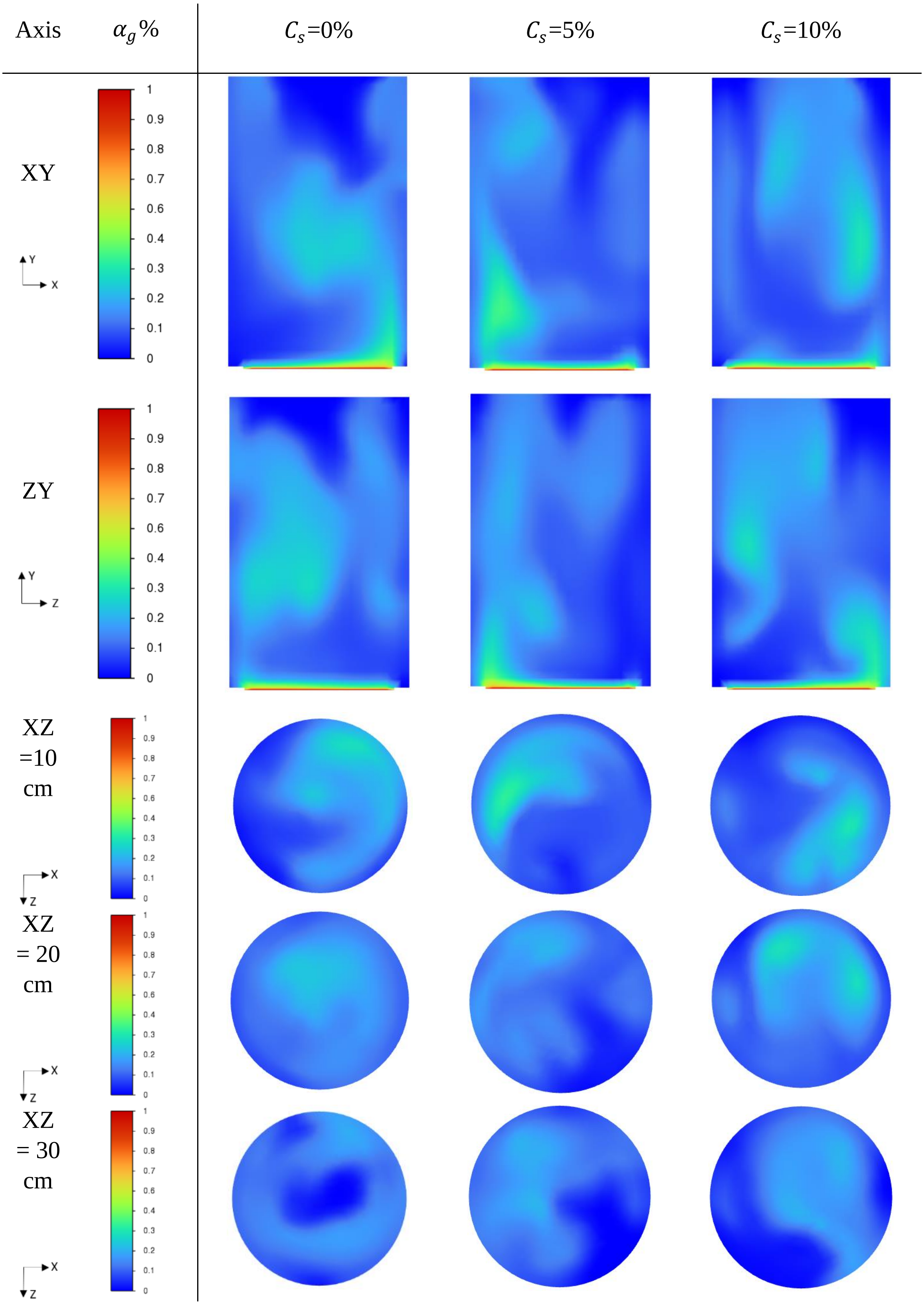

Fig. 5 Gas holdup contours for U_{gs}=0.05m/s for different solid particle concentrations.

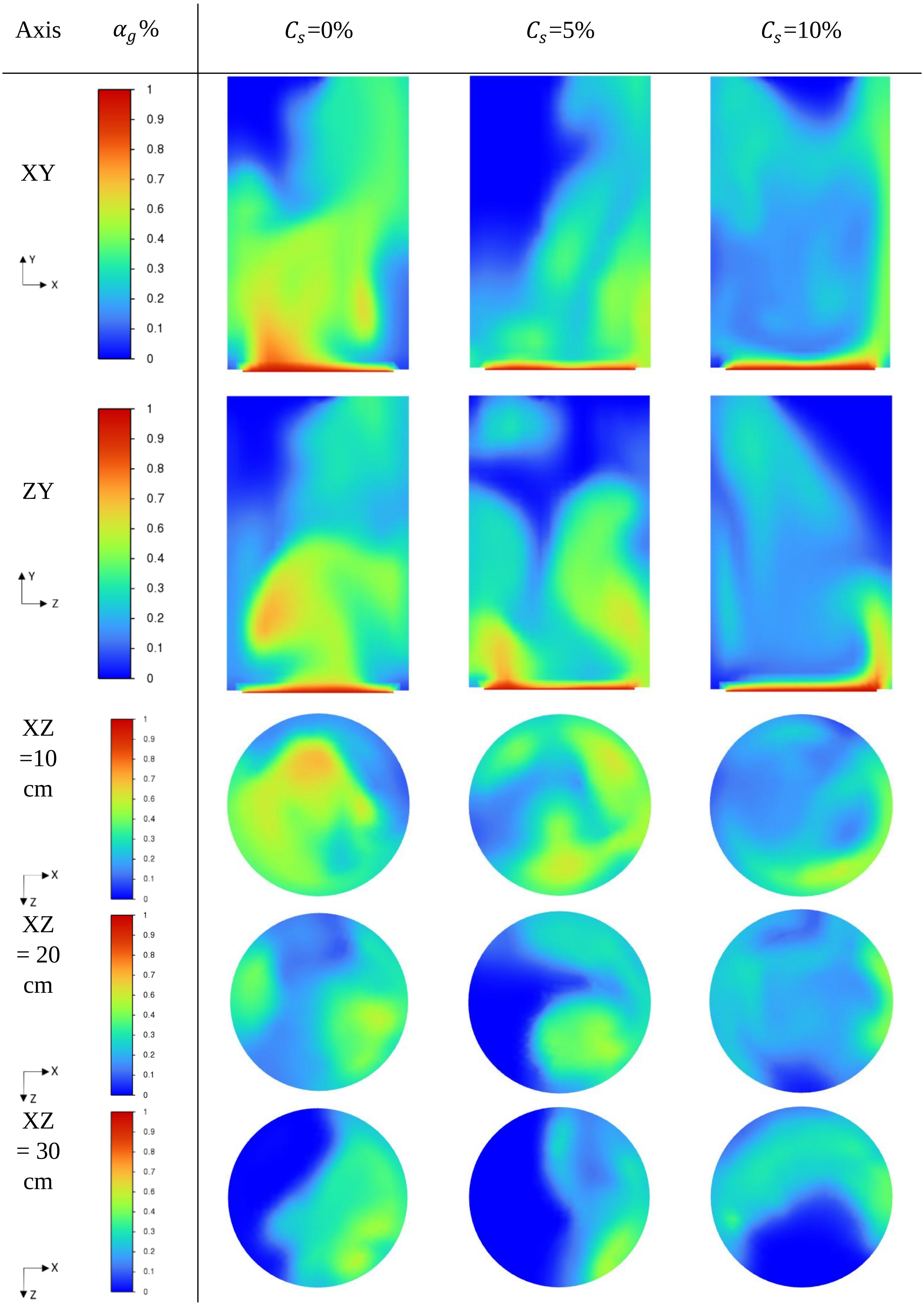

Fig. 6 Gas holdup contours for U_{gs}=0.15m/s for different solid particle concentrations.

The validation of gas holdup outcomes obtained from 3D-CFD Helium-Water-Alumina bubble column simulations was conducted by comparing them with experimental data from Abdulrahman [9] (see Fig. 8) and 2D simulations from Abdulrahman (see Fig. 9). The ability of the 3D-CFD models in identifying the gas holdup (α_g) at different solid concentrations is demonstrated in Figs. 8 and 9. Theoretical computational fluid dynamics (CFD) models in three dimensions have the capability to reasonably predict experimental data. The findings indicate that a significant proportion of gas holdup simulation outcomes were overestimated. One potential method for reducing relative error is to decrease the mesh size. A reduction in mesh size would enable the software to incorporate small vortical structures, such as eddies, into the flow analysis [26]. It has been observed that computational fluid dynamics (CFD) simulations exhibit greater accuracy in predicting simulations characterized by lower concentrations of solid particles. The investigation reveals that the highest relative percentage error is observed at $C_s = 10\%$, exhibiting an error of 8.37%. Subsequently, $C_s = 5\%$ exhibits a maximum error of 6.35%, while $C_s = 0\%$ demonstrates a maximum percentage error of 5.36%.

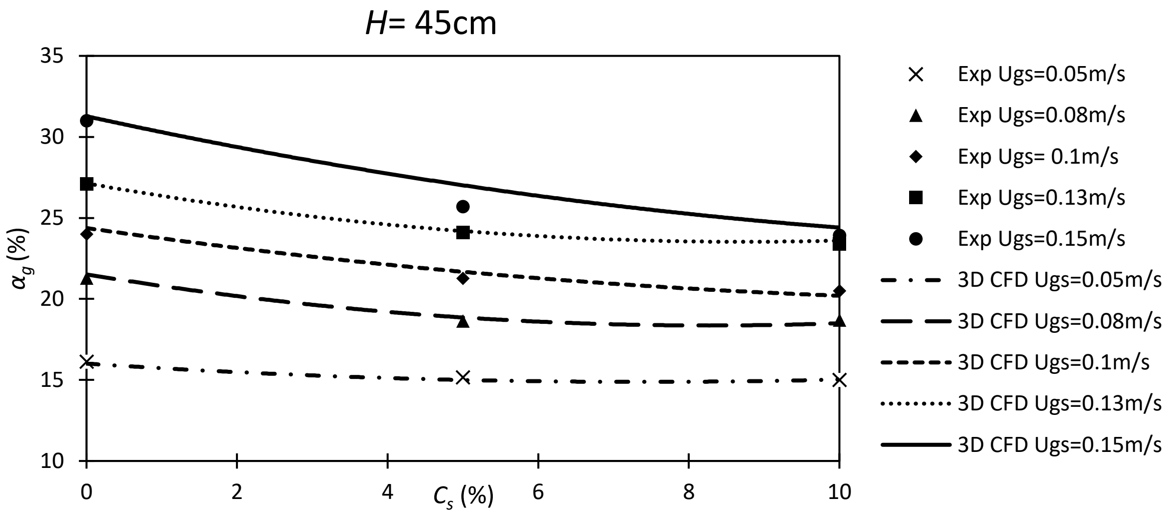

Fig. 7 Comparison of the average gas holdup versus solid particle concentration between 3D CFD simulations and experimental data.

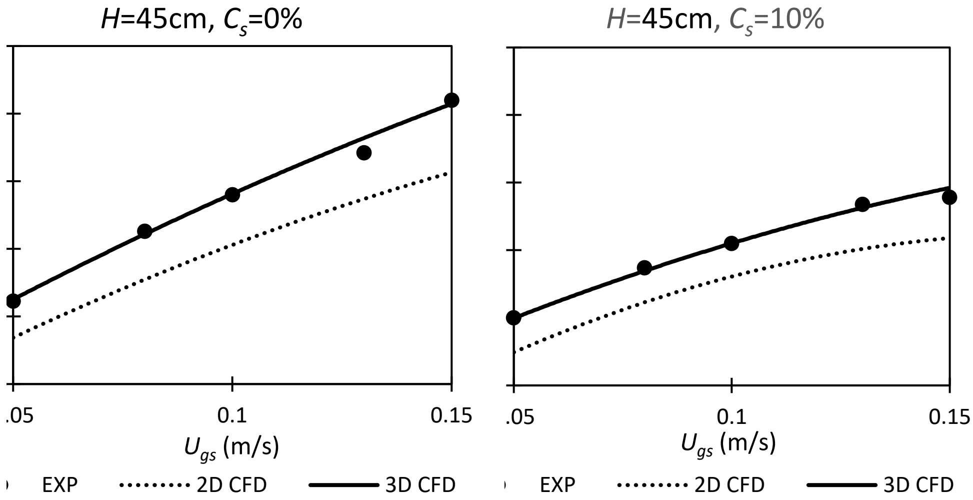

Fig. 8 Comparisons of the average gas holdup versus superficial gas velocity for different solid particle concentrations between 3D CFD simulations, 2D CFD simulations and experimental data.

5. Conclusions

The aim of this study is to investigate the hydrodynamic behavior of a direct contact heat transfer slurry bubble column reactor, wherein solid particle concentration effects are simulated using 3D-CFD. The reactor consists of a combination of helium gas and a slurry comprising liquid water and solid alumina particles. The findings indicate that the maximum percentage error for the gas holdup, when compared to experimental data, is 8.37%, specifically for a solid particle concentration of 10%. Nonetheless, in cases of reduced solid particle concentrations, specifically at 5% and 0%, the percentage error was comparatively lower, with values of 6.35% and 5.36%, respectively. It has been observed that a decrease in solid particle concentration leads to an increase in gas holdup. This phenomenon arises due to an increase of solid particle concentration, which results in an increase of the slurry viscosity. Increased viscosity result in the formation of large gas bubbles and a decrease in the rate of bubble breakdown. The higher velocity of the large bubbles will result in a reduction of the gas holdup. The aforementioned phenomenon has been noted within the Helium-Water-Alumina system under conditions of a static liquid height of 45 cm and a superficial gas velocity of 0.05m/s, where a decrease of 6% in gas holdup was observed upon increasing the C_s from 0% to 10%. In contrast to prior 2D computational fluid dynamics (CFD) simulations, the 3D CFD simulations presented in this study demonstrate enhanced precision. Specifically, the 3D simulation yielded a maximum percentage error of 8.37%, whereas the 2D simulations showed a maximum percentage error of 28.5%.

List of Symbols

A_i	al area concentration		field
C	heat		s of gas
	efficient		s of liquid
	diameter	U_{gs}	ial gas velocity
	ional acceleration		lup
		μ_{eff}	e viscosity
	erfacial forces between the phases	μ_g	c viscosity gas
	essure	μ_l	c viscosity liquid
$Q_{g,l}$	of heat exchange between the gas and liqui	ρ_g	gas
	s number	ρ_l	liquid
	ature	$\bar{\bar{\tau}}:\nabla V$	stress tensor contracted with the velocity

References

[1] Lewis, Michele A., Manuela Serban, and John K. Basco. "Hydrogen production at 550 ºC using a low temperature thermochemical cycle." *Proc. Nuclear Production of Hydrogen: Second Information Exchange Meeting*. 2003.

[2] Serban, Manuela, Michele A. Lewis, and John K. Basco. *Kinetic study of the hydrogen and oxygen production reactions in the copper-chloride thermochemical cycle*. American Institute of Chemical Engineers, 2004.

[3] Abdulrahman, Mohammed W. "Similitude for Thermal Scale-up of a Multiphase Thermolysis Reactor in the Cu-Cl Cycle of a Hydrogen Production." *International Journal of Energy and Power Engineering*, vol. 10.5, 2016, pp. 664-670.

[4] Abdulrahman, Mohammed W. "Heat Transfer Analysis of a Multiphase Oxygen Reactor Heated by a Helical Tube in the Cu-Cl Cycle of a Hydrogen Production." *International Journal of Mechanical and Mechatronics Engineering*, vol. 10.6, 2016, pp. 1122-1127.

[5] Abdulrahman, M. W., Wang, Z., Naterer, G. F., & Agelin-Chaab, M. "Thermohydraulics of a thermolysis reactor and heat exchangers in the Cu-Cl cycle of nuclear hydrogen production." in *Proceedings of the 5th World Hydrogen Technologies Convention*, 2013.

[6] Abdulrahman, Mohammed W. "Heat Transfer Analysis of the Spiral Baffled Jacketed Multiphase Oxygen Reactor in the Hydrogen Production Cu-Cl Cycle." In *Proceedings of the 9th International Conference on Fluid Flow, Heat and Mass Transfer (FFHMT'22)*, 2022.

[7] Abdulrahman, Mohammed W. "Review of the Thermal Hydraulics of Multi-Phase Oxygen Production Reactor in the Cu-Cl Cycle of Hydrogen Production." In *Proceedings of the 9th International Conference on Fluid Flow, Heat and Mass Transfer (FFHMT'22)*, 2022.

[8] Abdulrahman, Mohammed W. *Analysis of the thermal hydraulics of a multiphase oxygenproduction reactor in the Cu-Cl cycle*. Diss. University of Ontario Institute of Technology (Canada), 2016.

[9] Abdulrahman, Mohammed W., and Nibras Nassar. "Eulerian Approach to CFD Analysis of a Bubble Column Reactor–A." In *Proceedings of the 8th World Congress on Mechanical, Chemical, and Material Engineering (MCM'22)*, 2022.

[10] Abdulrahman, Mohammed W. "CFD Simulations of Gas Holdup in a Bubble Column at High Gas Temperature of a Helium-Water System." In *Proceedings of the 7th World Congress on Mechanical, Chemical, and Material Engineering (MCM'20)*, 2020

[11] Abdulrahman, M.W. "CFD Simulations of Direct Contact Volumetric Heat Transfer Coefficient in a Slurry Bubble Column at a High Gas Temperature of a Helium–Water–Alumina System." *Applied Thermal Engineering*, vol. 99, 2016, pp. 224–234.

[12] Abdulrahman, Mohammed W. "CFD Analysis of Temperature Distributions in a Slurry Bubble Column with Direct Contact Heat Transfer." In *Proceedings of the 3rd International Conference on Fluid Flow, Heat and Mass Transfer (FFHMT'16)*. 2016.

[13] Abdulrahman, Mohammed W. "Temperature profiles of a direct contact heat transfer in a slurry bubble column." *Chemical Engineering Research and Design*, vol. 182, 2022, pp. 183-193.

[14] Abdulrahman, Mohammed W. "Effect of Solid Particles on Gas Holdup in a Slurry Bubble Column." In *Proceedings of the 6th World Congress on Mechanical, Chemical, and Material Engineering*, 2020.

[15] Zhou, Rongtao, Ning Yang, and Jinghai Li. "A conceptual model for analyzing particle effects on gas-liquid flows in slurry bubble columns." *Powder Technology*, vol. 365, 2020, pp. 28-38.

[16] Wodołażski, Artur. "CFD Hydrodynamics Analysis of Syngas Flow in Slurry Bubble Column." *Journal of Oil, Gas and Petrochemical Technology*, vol. 3, no.1, 2016, pp. 83-96.

[17] Abdulrahman, M. W. "Experimental studies of gas holdup in a slurry bubble column at high gas temperature of a helium− water− alumina system." *Chemical Engineering Research and Design* vol. 109, 2016, pp. 486-494.

[18] Abdulrahman, M. W. "Experimental studies of the transition velocity in a slurry bubble column at high gas temperature of a helium–water–alumina system." *Experimental Thermal and Fluid Science*, vol. 74, 2016, pp. 404-410.

[19] Abdulrahman, M. W. "Experimental studies of direct contact heat transfer in a slurry bubble column at high gas temperature of a helium–water–alumina system." *Applied Thermal Engineering*, vol. 91, 2015, pp. 515-524.

[20] Abdulrahman, Mohammed Wassef. "Direct contact heat transfer in the thermolysis reactor of hydrogen production Cu—Cl cycle." U.S. Patent No. 10,059,586. 28 Aug. 2018.

[21] Abdulrahman, Mohammed Wassef. "Material substitution of cuprous chloride molten salt and oxygen gas in the thermolysis reactor of hydrogen production Cu—Cl cycle." U.S. Patent No. 10,526,201. 7 Jan. 2020.

[22] Abdulrahman, Mohammed W. "Simulation of Materials Used in the Multiphase Oxygen Reactor of Hydrogen Production Cu-Cl Cycle." *Proceedings of the 6 the International Conference of Fluid Flow, Heat and Mass Transfer (FFHMT'19)*. 2019.

[23] *ANSYS FLUENT Theory Guide*, Release 14.5. (2012). ANSYS, Inc.

[24] L. Schiller, A. Naumann, Uber die grundlegenden berechnungen bei der schwerkraftaufbereitung / About the basic calculations in the gravity-treatment, Zeitung des vereins deutscher ingenieure / Newspaper of the Association of German Engineers, 1933, pp. 77–318.

[25] Krishna, R., and S.T. Sie. “Design and Scale-up of the Fischer–Tropsch Bubble Column Slurry Reactor.” *Fuel Processing Technology*, vol. 64, no. 1-3, 2000, pp. 73–105.

[26] Sokolichin, A., and Gs Eigenberger. "Applicability of the standard k–ε turbulence model to the dynamic simulation of bubble columns: Part I. Detailed numerical simulations." *Chemical Engineering Science*, vol. 54, no. 13-14, 1999, pp. 2273-2284.